

Joint Flow Control, Routing and Medium Access Control in Random Access Multi-Hop Wireless Networks with Time Varying Link Capacities

Sucha Supittayapornpong¹ and Poompat Saengudomlert², Non-members

ABSTRACT

This work extends the existing static framework for joint flow control, routing and medium access control (MAC) in random access multi-hop wireless networks to a dynamic framework where link capacities vary over time. The overall problem is formulated as a long term network utility maximization (NUM) problem (instead of the existing static NUM problem) that accounts for link capacity variation. This dynamic formulation is more realistic than the static one, and is one step closer to practical networks. Under the stationary and ergodic assumptions on the link capacity variation, the problem is decomposed to form a distributed algorithm. The algorithm samples current link capacities while it is iteratively and locally updating flow rates and link transmission probabilities. Simulation results demonstrate the ability of the algorithm to sustain the optimal average data rates despite the link capacity variation.

Keywords: Network Optimization, Cross-Layer Optimization, Medium Access Control, Routing, Flow Control

1. INTRODUCTION

Multi-hop wireless networks are increasingly used as infrastructures, e.g., (mobile) wireless ad hoc networks and wireless sensor networks. To provide high data rates, efficient resource allocation schemes for multi-hop wireless networks are essential parts of the network architecture. While the traditional layered architecture can address these issues reasonably well for wireline networks, the nature of wireless medium makes the layered architecture inefficient since the layered architecture presumes separability of layers.

In wireless networks, resources are shared among layers with mechanisms from the physical layer to the transport layer that involve logical links. Due to the lack of central authority in typical wireless

multi-hop networks, random access medium access control (MAC) is considered. The end-to-end inefficiency of IEEE 802.11 MAC, which is based on random access and the traditional layered architecture, is demonstrated in [1,2] for multi-hop wireless networks. Several works attempt to improve the efficiency of the MAC mechanism [3-6]. A cross-layer design based on an optimization framework [7] for end-to-end efficiency is studied by Wang and Kar [8]. The work jointly designs flow control and MAC mechanisms with proportional fairness [9] in random access multi-hop wireless networks. Routing, which directly affects the resource allocation, is introduced to form the joint flow control, routing and MAC problem for a random access multi-hop network in [10]. However, in [10], all network parameters, including the topology and link capacities, are assumed static for the investigation.

In this work, we consider the joint design of flow control, routing and MAC in a random access multi-hop wireless network with link capacity variation. The system has a static network topology but dynamic link capacity variation. This variation has not been studied in all previously mentioned works, and is a step closer to a practical system. Using an optimization framework, a long term optimization formulation that accounts for changing of link capacities is formulated with an objective to provide proportional fairness among the rates of source-destination (S-D) pairs. To overcome a non-convexity of the formulation, a harmonic rate function is used while the routing is introduced into the formulation. In addition, stationary and ergodic assumptions of link capacity variation are considered. The formulation is then decomposed to form a distributed algorithm that requires link capacity parameters, link and flow costs, and flow rates. Only the parameters for link capacity variations are obtained from an environmental conditions using a stochastic approximation technique [11]. The other types are integrated inherently from the derived algorithm. Consequently, the formulation is solved by the distributed algorithm with a sampling mechanism.

The algorithm operates in two time scales which alternate between flow distribution and MAC mechanisms. The larger time scale corresponds to a MAC

Manuscript received on August 1, 2009 ; revised on October 1, 2009.

This work was supported by the Royal Thai Government (RTG) Fellowships.

^{1,2} The authors are with The Telecommunications Field of Study, Asian Institute of Technology, Thailand, E-mail: sucha.cpe@gmail.com and poompats@ait.ac.th

mechanism which adjusts link transmission probabilities at each node, while the smaller time scale corresponds to a flow distribution mechanism that adjusts flow rates at each source node. Both mechanisms sample channels for current link capacities subject to channel variation, and use them to adjust the probabilities and rates. The cooperation is done through the transmission probabilities and link prices introduced in the decomposition process.

Two set of simulation results show that the algorithm yields a system sustained at a global optimal solution based on the average link capacities regardless of the variation.

The rest of this paper is organized as follows. The system model and the joint flow control, routing and MAC problem are described in Section 2. The problem is decomposed in Section 3 to yield an algorithm in Section 4. Simulation results are given in Section 5. Section 6 concludes the work.

2. SYSTEM MODEL AND PROBLEM FORMULATION

2.1 Network Model

A multi-hop wireless network is represented by a directed graph $G(\mathcal{V}, \mathcal{E})$, where \mathcal{V} and \mathcal{E} denote the set of all nodes and the set of all logical directed links respectively. In what follows, we shall simply use the term “link” for “logical link”. A directed link $l = (t(l), r(l))$ exists between transmitter node $t(l)$ and receiver node $r(l)$ if $r(l)$ can reliably receive signals from $t(l)$.

End-to-end flows are denoted by their S-D pairs. Let \mathcal{S} denote the set of all predefined S-D pairs. An S-D pair $s \in \mathcal{S}$ is denoted by $(b(s), d(s))$ where $b(s)$ and $d(s)$ are the source and the destination of s . Each S-D pair has at least one path between its source and its destination. A path f of S-D pair s is defined as a set of directed links $\{l_1, \dots, l_k\}$ such that $t(l_1) = b(s)$, $r(l_k) = d(s)$, and $r(l_i) = t(l_{i+1})$ for all $i = 1, \dots, k-1$. We denote the set of all candidate paths of $s \in \mathcal{S}$ by $\mathcal{F}(f)$, and the set of all paths in a network by $\mathcal{F} = \bigcup_f \mathcal{F}(f)$. For each path f , let $\mathcal{L}(f) = \{l | l \in f\}$ denote the set of all links contained in f . On the other hand, let $\mathcal{R}(l) = \{f \in \mathcal{F} | l \in \mathcal{L}(f)\}$ denote the set of all paths on link l . Define link $l \in \mathcal{E}$ to be active if $\mathcal{R}(l)$ is not empty. Let $\mathcal{L} \subset \mathcal{E}$ be the set of all active links. Node $n \in \mathcal{V}$ is active if there exists an $l \in \mathcal{L}$ such that $n = t(l)$ or $n = r(l)$. Let $\mathcal{N} \subset \mathcal{V}$ denote the set of all active nodes. For convenience, we define the active graph $A(\mathcal{N}, \mathcal{L})$. This graph consists of only nodes and links involved in the calculation of this work.

At a node level, each active node $n \in \mathcal{N}$ has the set of outgoing links and the set of incoming links denoted respectively as $\mathcal{O}(n) = \{l \in \mathcal{L} | t(l) = n\}$ and $\bar{\mathcal{O}}(n) = \{l \in \mathcal{L} | r(l) = n\}$. For each active node $n \in \mathcal{N}$, let the set of all one-hop active nodes with respect to n be denoted by $\mathcal{H}(n) = \{t(l) \in \mathcal{N} | r(l) = n, l \in \mathcal{E}\}$.

Note that an active node in $\mathcal{H}(n)$ and node n may have either an active link in \mathcal{L} or an inactive link in \mathcal{E} between them. In addition, a transmission by an active node in $\mathcal{H}(n)$ can potentially interfere with a reception at node n .

We assume symmetrical transmission ranges, i.e., a transmitter can reach to a receiver if and only if the receiver can reach the transmitter. Because a collision occurs at a receiver of a link when the receiver node receives signals from multiple links or when the receiver node transmits while there is an incoming signal. Let $\mathcal{I}(l) = \mathcal{H}(r(l)) \cup \{r(l)\} - \{t(l)\}$ denote the set of all active nodes that may cause an unsuccessful transmission to link l . Let $\bar{\mathcal{I}}(n) = \left(\bigcup_{k \in \mathcal{H}(n) \cup \{n\}} \bar{\mathcal{O}}(k) \right) - \mathcal{O}(n)$ denote the set of all active links that may be interfered by a transmission of node n .

2.2 Time Varying Link Capacity

In the dynamic environment that we shall consider, the physical layer adapts to link quality variation and the overall effect is variation in link capacities. Our model mimics the IEEE 802.11b physical layer that has four link capacity states. Nevertheless, this assumption can be extended to any other finite number of states. The capacity of each link $l \in \mathcal{L}$ (in Mbps) is modeled by a discrete stochastic process $\{C_l(\omega_l, t), t \geq 0\}$ where ω_l is an outcome in sample space Ω_l and t denotes the slot time. At slot time t , the state $C_l(\omega_l, t)$ is in the set $\Psi = \{11, 5.5, 2, 1\}$. We assume that all link capacities are independent.

2.3 Average Link Rate

As in [10], slotted Aloha [12] is considered for tractability. In each slot, every active node $n \in \mathcal{N}$ transmits with node transmission probability $P^{(n)}$, $0 \leq P^{(n)} \leq 1$. Let $0 \leq p_l \leq 1$ denote the link transmission probability of link $l \in \mathcal{L}$. The node transmission probability is divided to its outgoing link transmission probabilities with $P^{(n)} = \sum_{l \in \mathcal{O}(n)} p_l$. Let $\mathbf{p} = (p_l : l \in \mathcal{L})$ be a vector of all link transmission probabilities with the feasible set \mathcal{P} defined by

$$\mathcal{P} = \left\{ \mathbf{p} \left| \begin{array}{ll} \sum_{h \in \mathcal{O}(n)} p_h \leq 1 & \text{for all } n \in \mathcal{N} \\ 0 \leq p_l \leq 1 & \text{for all } l \in \mathcal{L} \end{array} \right. \right\}. \quad (1)$$

Since a collision occurs at a receiver node of each active link if the node receives signals from multiple transmitting nodes or the node is transmitting as well as receiving, a successful transmission probability [4-6,8,10] of link l is

$$\phi_l(\mathbf{p}) = p_l \prod_{k \in \mathcal{I}(l)} (1 - P^{(k)}).$$

Hence, the average link rate $\Phi_l(C_l(\omega_l, t), \mathbf{p})$ of link l is defined by

$$\Phi_l(C_l(\omega_l, t), \mathbf{p}) = C_l(\omega_l, t)\phi_l(\mathbf{p}). \quad (2)$$

2.4 Fairness and Harmonic Rate

To overcome the non-convexity of the associated optimization problem and to provide proportional fairness [9] between S-D pairs, the harmonic rate function proposed in [10] is used at each S-D pair to represent the S-D pair's rate in a one dimensional scale. A rate of S-D pair s with the harmonic rate function is [10]

$$\chi(\mathbf{y}_s) = |\mathbf{y}_s|^2 \left/ \sum_{i=1}^{|\mathbf{y}_s|} y_i^{-1} \right.$$

where y_f denotes the flow rate on path f and $\mathbf{y}_s = (y_f : f \in \mathcal{F}(s))$ denotes a vector of flow rates of S-D pair s .

To provide proportional fairness, the utility of S-D pair s is set equal to the log-harmonic rate of its flows \mathbf{y}_s , which is

$$U_s = \log \left(|\mathcal{F}(s)|^2 \left/ \sum_{f \in \mathcal{F}(s)} y_f^{-1} \right. \right) \quad (3)$$

where $|A|$ denotes the cardinality or dimension of A . The characteristics of the log-harmonic rate function are studied in [10], where it is shown that using the log-harmonic rate provides a fairer treatment among S-D pairs compared to viewing different paths of the same S-D pair as virtually separated S-D pairs. Furthermore, flows of an S-D pair tend to be distributed more equally among its candidate paths.

2.5 Optimization Formulation

The design of joint flow control, routing and MAC in slotted Aloha multi-hop wireless networks is formulated as a long term network utility maximization (NUM) problem that accounts for the variation of link capacities. Its objective is to maximize the aggregate end-to-end log-harmonic rates in (3) among S-D pairs each of which has multiple candidate paths. Since a constant in the objective function can be ignored, the joint flow control, routing and MAC formulation is formulated as

$$\text{Maximize} \quad \sum_{s \in \mathcal{S}} -\log \left(\sum_{f \in \mathcal{F}(s)} y_f^{-1} \right) \quad (4)$$

$$\begin{aligned} \text{Subject to} \quad & \sum_{f \in \mathcal{R}(l)} y_f \leq \\ & \lim_{T \rightarrow \infty} \frac{1}{T} \sum_{t=1}^T \Phi_l(C_l(\omega_l, t), \mathbf{p}) \quad \forall l \in \mathcal{L} \\ & \mathbf{y} \in \mathbb{R}_+^{|\mathcal{F}|}, \quad \mathbf{p} \in \mathcal{P} \end{aligned}$$

where \mathbb{R}_+ is the non-negative real number set and $\mathbf{y} = (y_f : f \in \mathcal{F})$ is a vector of all flow rates.

The first constraint in (4) is a link capacity constraint where the aggregate rate of all candidate paths using the link cannot exceed the long term average of the link rate defined in (2). The second constraint is to ensure the non-negativity of all flow rates and the feasibility of all link transmission probabilities defined in (1).

Mathematically, formulation (4) can possibly be solved after all the information is known (for each time slot). However, in practice, it is not possible to wait for this information before the system starts operating. We then consider the formulation under stationary and ergodic assumptions. With these assumptions, the time index t from $\mathbb{E}_\Psi[C_l(\omega_l, t), \mathbf{p}]$ can be dropped. Thus, the formulation under these assumptions is

$$\text{Maximize} \quad \sum_{s \in \mathcal{S}} -\log \left(\sum_{f \in \mathcal{F}(s)} y_f^{-1} \right) \quad (5)$$

$$\begin{aligned} \text{Subject to} \quad & \sum_{f \in \mathcal{R}(l)} y_f \leq \Phi_l(\mathbb{E}_\Psi[C_l(\omega_l)], \mathbf{p}) \quad \forall l \in \mathcal{L} \\ & \mathbf{y} \in \mathbb{R}_+^{|\mathcal{F}|}, \quad \mathbf{p} \in \mathcal{P} \end{aligned}$$

where $\mathbb{E}_\Psi[\cdot]$ is the expectation taken over the set Ψ . Note that the long term NUM is inspired by the work from O'Neill's group [13].

Formulation (5) is non-convex since the first constraint yields a non-convex feasible set. However, it can be transformed to a convex optimization formulation stated in Theorem 1. It is done by changing $y_f = e^{z_f}$ for all $f \in \mathcal{F}$, taking the logarithm on both sides of the first constraint of formulation (5)

Theorem 1. *The following optimization problem is convex.*

$$\text{Maximize} \quad \sum_{s \in \mathcal{S}} -\log \left(\sum_{f \in \mathcal{F}(s)} e^{-z_f} \right) \quad (6)$$

$$\begin{aligned} \text{Subject to} \quad & \log \sum_{f \in \mathcal{R}(l)} e^{z_f} \leq \\ & \log \Phi_l(\mathbb{E}_\Psi[C_l(\omega_l)], \mathbf{p}) \quad \forall l \in \mathcal{L} \\ & \mathbf{z} \in \mathbb{R}^{|\mathcal{F}|}, \quad \mathbf{p} \in \mathcal{P}, \end{aligned}$$

where \mathbb{R} is the real number set and $\mathbf{z} = (z_f : f \in \mathcal{F})$.

Proof: See Appendix 1.

3. DECOMPOSITION

Formulation (6) can be solved by a centralized solver; however, it can also be solved distributively using vertical decomposition and horizontal decomposition. Both decompositions are respectively done in order to reduce the problem's complexity and to solve the problem distributively.

A separable formulation is obtained from the convex formulation in (6) by removing logarithm functions from the link capacity constraints. Thus, the separable problem is

$$\begin{aligned} & \text{Maximize} && \sum_{s \in \mathcal{S}} -\log \left(\sum_{f \in \mathcal{F}(s)} e^{-z_f} \right) \\ & \text{Subject to} && \sum_{f \in \mathcal{R}(l)} e^{z_f} \leq \Phi_l(\mathbb{E}_\Psi[\mathcal{C}_l(\omega_l)], \mathbf{p}) \quad \forall l \in \mathcal{L} \\ & && \mathbf{z} \in \mathbb{R}^{|\mathcal{F}|}, \quad \mathbf{p} \in \mathcal{P} \end{aligned} \quad (7)$$

Formulation (7) is non-convex. However, it is needed for computation because of the separable property of its link capacity constraint. The following theorem states a relation between formulations (6) and (7).

Theorem 2. *A local optimal solution that satisfies the first-order necessary optimality condition [14] of formulation (7) is a local optimal solution that satisfies the first-order necessary optimality condition of formulation (6).*

Proof: See Appendix 2.

Since formulation (6) is convex, a solution that satisfies the KKT conditions is a global optimal solution of formulation (6). Therefore, a local optimal solution of formulation (7) yields a global optimal solution of formulation (6). Indeed, finding a local optimal solution of formulation (7) yields a global optimal solution of formulation (6).

3.1 Vertical Decomposition

Formulation (7) is firstly vertically decomposed [7] to the MAC problem and the flow distribution (FD) problem. Note that, in what follows, the term “formulation” and “problem” are used interchangeably.

The MAC problem, which adjusts only link transmission probabilities, i.e., \mathbf{p} , is

$$\begin{aligned} & \text{Maximize} && \mathbf{Q}(\mathbf{p}) \\ & \text{Subject to} && \mathbf{p} \in \mathcal{P} \end{aligned} \quad (8)$$

where \mathbf{p} is the only variable in problem (8) and $\mathbf{Q}(\mathbf{p})$ is the optimal cost of the FD problem to be described next. The FD problem is a subroutine in problem (8) and returns its optimal value back to problem (8).

The FD problem, which adjusts only flow rates, i.e., \mathbf{z} , is defined as

$$\begin{aligned} & \text{Maximize} && \sum_{s \in \mathcal{S}} -\log \left(\sum_{f \in \mathcal{F}(s)} e^{-z_f} \right) \\ & \text{Subject to} && \sum_{f \in \mathcal{R}(l)} e^{z_f} \leq \Phi_l(\mathbb{E}_\Psi[\mathcal{C}_l(\omega_l)], \mathbf{p}) \quad \forall l \in \mathcal{L} \\ & && \mathbf{z} \in \mathbb{R}^{|\mathcal{F}|} \end{aligned} \quad (9)$$

In problem (9), vector \mathbf{z} is a variable, but \mathbf{p} is fixed as a constant parameter of the problem. We emphasize the the optimal cost $\mathbf{Q}(\mathbf{p})$ is a function of \mathbf{p} . For this reason, the feasible set of the problem becomes convex since the right side of the first constraint is a constant and the left side is a sum of exponential functions, which is a convex function. The problem’s objective is convex because it maximizes a concave function as proved in Lemma 1 in Appendix 1.

Note that, from problems (8) and (9), the FD problem is a subroutine in the MAC problem. After horizontal decomposition, as a consequence, the FD problem leads to a smaller time scale mechanism, whereas the MAC problem leads to a larger time scale mechanism.

3.2 Horizontal Decomposition

Instead of solving (8) and (9) by centralized schemes, the two problems are horizontally decomposed [7] and solved distributively. This is done to derive a distributed algorithm for formulation (5).

Flow Distribution Mechanism

The FD problem is a convex optimization problem in which the Slater condition [14] holds. Therefore, it can be solved by its dual problem. Let $\lambda_l \geq 0$ denote a dual variable corresponding to the capacity constraint of link $l \in \mathcal{L}$, and define $\boldsymbol{\lambda} = (\lambda_l : l \in \mathcal{L})$. The Lagrangian of problem (9) is

$$\begin{aligned} L(\mathbf{z}, \boldsymbol{\lambda}) &= \sum_{s \in \mathcal{S}} B(s) + \sum_{l \in \mathcal{L}} \lambda_l \left(\Phi_l(c_l, \mathbf{p}) - \sum_{f \in \mathcal{R}(l)} e^{z_f} \right) \\ &= \sum_{s \in \mathcal{S}} B(s) + \sum_{l \in \mathcal{L}} \lambda_l \Phi_l(c_l, \mathbf{p}) - \sum_{f \in \mathcal{F}} e^{z_f} \bar{\lambda}(f) \\ &= \sum_{s \in \mathcal{S}} \left[B(s) - \sum_{f \in \mathcal{F}(s)} e^{z_f} \bar{\lambda}(f) \right] + \sum_{l \in \mathcal{L}} \lambda_l \Phi_l(c_l, \mathbf{p}), \end{aligned}$$

where $B(s) = -\log \left(\sum_{f \in \mathcal{F}(s)} e^{-z_f} \right)$, $\bar{\lambda}(f) = \sum_{l \in \mathcal{L}(f)} \lambda_l$ and $c_l = \mathbb{E}_\Psi[\mathcal{C}_l(\omega)]$. Intuitively, λ_l can be interpreted as a price of link l , and $\bar{\lambda}(f)$ is a price of flow f .

The dual function of problem (9) is to find

$$\begin{aligned} D(\boldsymbol{\lambda}) &= \max_{\mathbf{z}} L(\mathbf{z}, \boldsymbol{\lambda}) \\ &= \max_{\mathbf{z}} \sum_{s \in \mathcal{S}} \left[B(s) - \sum_{f \in \mathcal{F}(s)} e^{z_f} \bar{\lambda}(f) \right] + \sum_{l \in \mathcal{L}} \lambda_l \Phi_l(c_l, \mathbf{p}) \\ &= \sum_{s \in \mathcal{S}} \max_{\mathbf{z}(s)} \left[B(s) - \sum_{f \in \mathcal{F}(s)} e^{z_f} \bar{\lambda}(f) \right] + \sum_{l \in \mathcal{L}} \lambda_l \Phi_l(c_l, \mathbf{p}), \end{aligned} \quad (10)$$

where $\mathbf{z}(s) = (z_f : f \in \mathcal{F}(s))$ is a vector of transformed flow rates. Therefore, we can distributively

solve for \mathbf{z} in 10 at each source node. Each source s requires $\bar{\lambda}(f)$, $f \in \mathcal{F}(s)$, from the source's flows, and then calculate

$$\hat{\mathbf{z}}^{[j]}(s) = \underset{\mathbf{z}(s)}{\operatorname{argmax}} \left(B(s) - \sum_{f \in \mathcal{F}(s)} e^{z_f} \bar{\lambda}^{[j]}(f) \right), \quad (11)$$

where $a^{[j]}$ denotes scalar or vector a at iteration j .

The dual problem is

$$\begin{aligned} & \text{Minimize} && D(\boldsymbol{\lambda}) \\ & \text{Subject to} && \boldsymbol{\lambda} \geq \mathbf{0}. \end{aligned}$$

It's objective function is a pointwise maximum function; therefore, a subgradient method [14] can be used to solve the problem. However, the system does not know $\mathbb{E}_{\Psi} [C_l(\omega_l)]$. To overcome this issue, a stochastic approximation technique [14] is applied. In this technique, we approximate the gradient of $D(\boldsymbol{\lambda})$ with respect to λ_l , $l \in \mathcal{L}$ by using the actual observation $C_l^{[j]}(\omega_l)$ instead of its mean $\mathbb{E}_{\Psi} [C_l(\omega_l)]$. Consequently, the method samples current link capacities and performs the following iterative computation at each link l

$$\lambda_l^{[j+1]} = \left[\lambda_l^{[j]} - \gamma^{[j]} \left(\Phi_l \left(C_l^{[j]}(\omega_l), \mathbf{p} \right) - \sum_{f \in \mathcal{R}(l)} e^{\hat{z}_f^{[j]}} \right) \right]^+ \quad (12)$$

where $[\cdot]^+$ denotes a projection on a feasible non-negative set, γ denotes the step size and $C_l^{[j]}(\omega_l)$ is the sampled capacity of link l at time step j . The update condition (12) at link l requires \hat{z}_f , $f \in \mathcal{R}(l)$, from every flow over it. We denote an optimal dual solution from $\mathbf{Q}^{[i]}(\mathbf{p}^{[i]})$ as $\lambda^{*[i]}$.

MAC Mechanism

To solve problem (8), \mathbf{p} is updated in the gradient direction of the objective function. Using a stochastic approximation technique [11], the associated gradient projection method [14] is

$$p_l^{[i+1]} = \left[p_l^{[i]} + \beta^{[i]} \frac{\partial \mathbf{Q}^{[i]}(\mathbf{p}^{[i]})}{\partial p_l} \right]^{\mathcal{P}^{(i)}}, \quad (13)$$

where β is the step size and $[\cdot]^{\mathcal{P}^n}$ is the projection to a feasible set

$$\mathcal{P}^n = \left\{ \mathbf{p}_n \mid \begin{array}{l} \sum_{h \in \mathcal{O}(n)} p_h \leq 1 \\ 0 \leq p_l \leq 1 \end{array} \text{ for all } l \in \mathcal{O}(n) \right\}$$

and $\mathbf{p}_n = (p_l : l \in \mathcal{O}(n))$.

The term $\frac{\partial \mathbf{Q}^{[i]}(\mathbf{p}^{[i]})}{\partial p_l}$ is derived from the sensitivity theorem [14] as

$$\begin{aligned} & \frac{\partial \mathbf{Q}^{[i]}(\mathbf{p}^{[i]})}{\partial p_l} \\ &= \sum_{h \in \mathcal{L}} \frac{\partial \mathbf{Q}^{[i]}(\mathbf{p}^{[i]})}{\partial \Phi_h \left(C_h^{[i]}(\omega_h), \mathbf{p}^{[i]} \right)} \cdot \frac{\partial \Phi_h \left(C_h^{[i]}(\omega_h), \mathbf{p}^{[i]} \right)}{\partial p_l} \\ &= \sum_{h \in \mathcal{L}} \lambda_h^{*[i]} \frac{\partial \Phi_h \left(C_h^{[i]}(\omega_h), \mathbf{p}^{[i]} \right)}{\partial p_l} \end{aligned}$$

when

$$\frac{\partial \Phi_h \left(C_h^{[i]}(\omega_h), \mathbf{p}^{[i]} \right)}{\partial p_l} = \begin{cases} C_l^{[i]}(\omega_l) \prod_{k \in \mathcal{I}(l)} (1 - P^{(k)}) & , h = l \\ -C_h^{[i]}(\omega_h) p_h \prod_{k \in \mathcal{I}(h) - \{t(l)\}} (1 - P^{(k)}) & , h \in \bar{\mathcal{I}}(n) \end{cases}$$

which requires two-hop local information $p_h, P^{(t(h))}$, $h \in \bar{\mathcal{I}}(t(l))$. Thus, the update condition (13) is performed at each link by the transmitter node from the two-hop local information.

4. ADAPTIVE ALGORITHM

The problem decomposition yields an adaptive algorithm that involves iterative solving of the MAC problem (8) and the FD problem (9) in two time scales. In the larger time scale, the MAC mechanism distributively adjusts p_l by using two-hop local information of $P^{(n)[i]}, n \in \bigcup_{j \in \mathcal{I}(t(l))} \mathcal{I}(j) - \{t(l)\}$ and $p_h^{[i]}, C_h^{[i]}(\omega_h), \lambda_h^{*[i]}, h \in \bar{\mathcal{I}}(t(l))$. In the smaller time scale, the FD mechanism distributively calculates an intermediate $\hat{\mathbf{z}}(s)$ using local information $\bar{\lambda}^{[j]}(f), f \in \mathcal{F}(s)$, then adjusts λ_l using local information $\hat{z}_f^{[j]}, f \in \mathcal{R}(l)$. The values of $C_l^{[i]}(\omega_l)$, $l \in \mathcal{L}$, are obtained from sampling at iteration i on every link $l \in \mathcal{L}$. A process alternates between the small time scale and the large time scale until the system converges. The overall distributed algorithm is summarized as follows.

We assume that predefined candidate paths are obtained from some routing algorithm in the network layer. Then, the adaptive distributed algorithm for joint flow control, routing and MAC in random access multi-hop wireless networks with link capacity variation is summarized in Fig. 1.

Note that the computation of each link can be performed by its transmitter node. If the algorithm is supposed to run forever, step 19 is changed to "Repeat 3 to 19", and step 20 is discarded.

5. SIMULATION RESULTS

The simulation is implemented in Python. We use a four-state Markov chain shown in Fig 2 to generate

Joint Flow Control, Routing and MAC Adaptive Distributed Algorithm	
1:	Each node $n \in \mathcal{N}$ and link $l \in \mathcal{L}$ construct their local sets $\mathcal{O}(n)$, $\mathcal{I}(n)$, $\mathcal{I}(l)$.
2:	Each link $l \in \mathcal{L}$ sets its initial values of p_l and λ_l .
3:	MAC-loop (iteration index i)
4:	FD-loop (iteration index j)
5:	At each source $s \in \mathcal{S}$
6:	Collect the price $\bar{\lambda}^{[j]}(f)$, $f \in \mathcal{F}(s)$ from its links (denoted by $\mathcal{L}(f)$).
7:	Compute new $\mathbf{z}^{[j]}(s)$ from (11).
8:	Distribute new $z_f^{[j]}$ to links in $\mathcal{L}(f)$, $f \in \mathcal{F}(s)$.
9:	At each link $l \in \mathcal{L}$
10:	Sample current ideal link capacity $C_l^{[j]}(\omega_l)$.
11:	Compute new price $\lambda_l^{[j+1]}$ from (12).
12:	Repeat 4 to 11 until $\boldsymbol{\lambda}$ converges, which yields $\boldsymbol{\lambda}^*$ and \mathbf{z}^* .
13:	Each source $s \in \mathcal{S}$ sets its flow rates $y_f = e^{z_f^*}$, $f \in \mathcal{F}(s)$.
14:	Each link $l \in \mathcal{L}$ sets its price $\lambda_l^{*[i]} = \lambda_l^*$.
	End FD-loop
15:	At each link $l \in \mathcal{L}$
16:	Sample local current ideal link capacity $C_l^{[i]}(\omega_l)$.
17:	Collect local node, link probabilities, sampled capacities, and prices as $P^{(n)}, p_h, C_h^{[i]}(\omega_h), \lambda_h^{*[i]}$ where $n \in \bigcup_{j \in \bar{\mathcal{I}}(t(l))} \mathcal{I}(j) - \{t(l)\}$ and $h \in \bar{\mathcal{I}}(t(l))$.
18:	Compute new $p_l^{[i+1]}$ from (13).
19:	Repeat 3 to 19 until \mathbf{p} converges.
	End MAC-loop
20:	Algorithm terminates.

Fig.1: Overall Algorithm for Joint Flow Control, Routing, And Medium Access Control

link capacity variations [15].

From Fig. 2, let C11, C5.5, C2 and C1 be the first, second, third and fourth states respectively. Each link has a transition matrix T defined for its Markov chain. Each element $T_{i,j}$ in T represents the transition probability from state i to state j . Since every link is independent, each link may have a different transition matrix; however, for simplicity in the simulation process, we define a common transition matrix T for every link as shown in Fig. 2.

All parameters and conditions of the distributed algorithm in simulation are described below. Initialized variables are $p_l = 0.1$ and $\lambda_l = 1$ for all $l \in \mathcal{L}$, and $z_f = -\infty$ for all $f \in \mathcal{F}$. The step size in (12) and (13) are specified in each simulation. For the purpose of simulation, the convergence threshold of the FD problem (9) is $T_{FC} = 5 \times 10^{-3}$, and the problem terminates when $T_{FC} \geq \max_{l \in \mathcal{L}} |\Delta \lambda_l|$, where Δa is the difference in quantity a between successive iterations. The convergence threshold of the MAC problem (8) is $T_{MAC} = 10^{-7}$, and the problem terminates when $T_{MAC} \geq \max_{l \in \mathcal{L}} |\Delta p_l|$. The flow distribution problem has a reducing step size mechanism [14] with the condition $\gamma^{[j]} = \gamma/j$ for some constant $\gamma > 0$. Variable $\hat{\mathbf{z}}$ in (11) is solved by a solver from the CVXOPT module in Python.

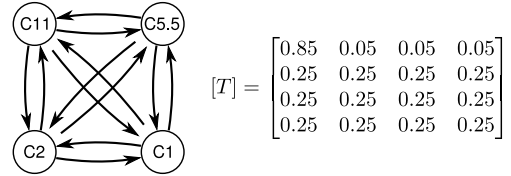


Fig.2: Markov Chain for Link Capacity Variation

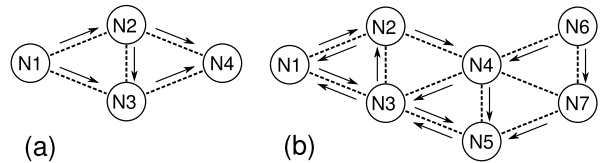


Fig.3: Example Networks Used in Simulation

5.1 Simple Network

The simple network topology used for simulation is illustrated in Fig. 3a. S-D pair ($N1:N4$) has candidate paths $[N1, N2, N4]$ and $[N1, N3, N4]$. S-D pair ($N2:N4$) has candidate paths $[N2, N3, N4]$ and $[N2, N4]$. The simulation sets $\beta^{[i]} = 1 \times 10^{-3}$ and $\gamma = 1 \times 10^{-1}$. We also solve convex formulation (6) directly using a solver in Octave. The optimal results are shown in Table 1.

Results from an algorithm with static link capacity [10] are also listed in Table 1, and match the results from the centralized Octave solver. In particular, static link capacities are set equal to the average

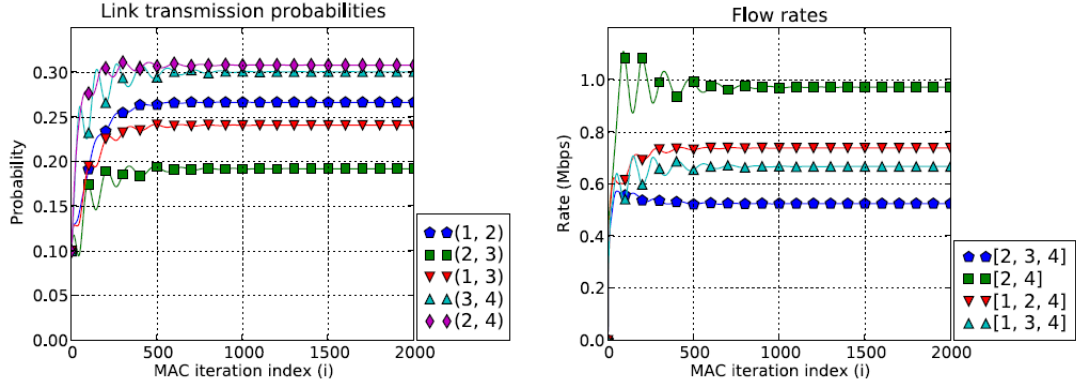


Fig.4: Simple Network Results without Link Capacity Variation

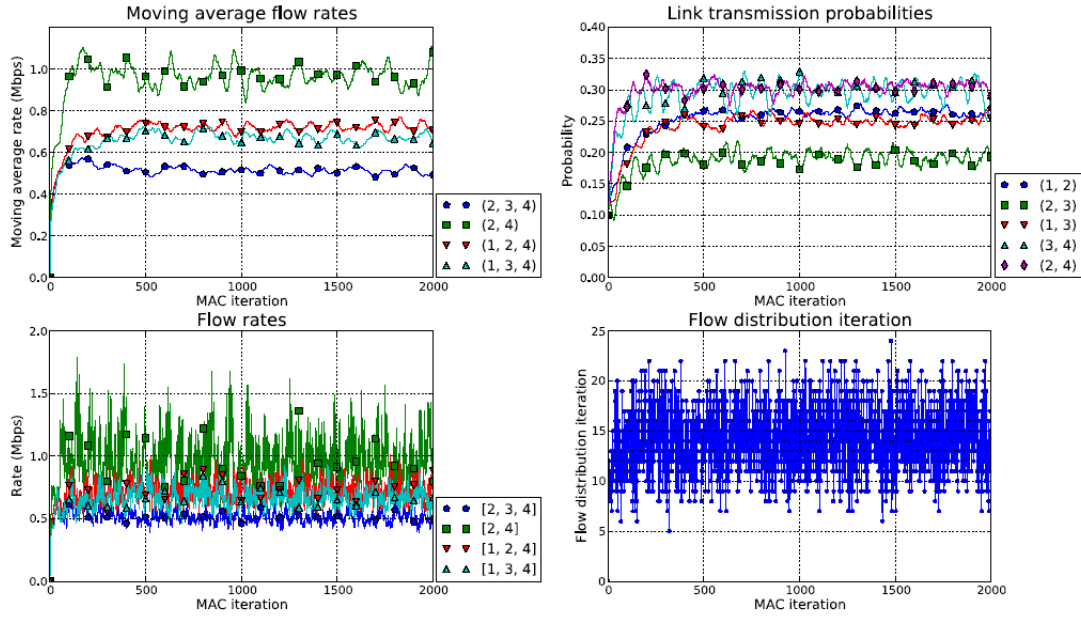


Fig.5: Simple Network Results with Link Capacity Variation

Table 1: Solutions from A Simple Network

Variable	Static link capacities		Varying link capacities
	Centralized	Distributed	Distributed
S-D rates			
(N1:N4)	1.406	1.407	1.347
(N2:N4)	1.498	1.498	1.573
Flow rates			
[N1, N2, N4]	0.738	0.739	0.705
[N1, N3, N4]	0.668	0.668	0.642
[N2, N3, N4]	0.525	0.525	0.492
[N2, N4]	0.973	0.973	1.081
Link transmission probabilities			
(N1, N2)	0.267	0.267	0.272
(N1, N3)	0.241	0.241	0.241
(N2, N3)	0.192	0.192	0.193
(N2, N4)	0.308	0.308	0.305
(N3, N4)	0.301	0.301	0.295

link capacities. This implies that the algorithm converges to an optimal solution. Evolution of the algorithm, link transmission probabilities and flow rates, is illustrated in Fig. 4.

With link capacity variation, the proposed algorithm's performances, which are link transmission probabilities, flow rates, average flow rate, and numbers of FD problem's iteration, are plotted in Fig. 5, and their results after the 2000th iteration are listed in Table 1. The average flow rates are calculated from an average of consecutive 64 data points. Compared with the results without variation, the algorithm sustains approximately the same average flow rates regardless of the variation.

The fairness among S-D pairs follows the static formulation in [10] as mentioned in Section 2.4.

5.2 More Complex Network

A more complex network topology is illustrated in Fig. 3b. S-D pair (N1:N5) has candidate

paths $[N1, N2, N4, N5]$ and $[N1, N3, N5]$. S-D pair $(N3:N1)$ has candidate paths $[N3, N1]$ and $[N3, N2, N1]$. S-D pair $(N6:N3)$ has candidate paths $[N6, N4, N3]$ and $[N6, N7, N5, N3]$. The simulation sets $\beta^{[i]} = 5 \times 10^{-5}$ and $\gamma = 1 \times 10^{-1}$. The results, which are link transmission probabilities, flow rates, average flow rates, and numbers of FD problem's iteration, are illustrated in Fig. 6. This example demonstrates the applicability of the algorithm in a more complex network.

6. CONCLUSION

We have jointly designed a cross-layer flow control, routing and MAC mechanism for random access multi-hop wireless networks with link capacity variation. Under the stationary and ergodic assumptions of the link capacity variation, the distributed algorithm has been derived based on decomposition of the underlying optimization problem in dynamic environments. Simulation results show that the algorithm can sustain the flow rates equal to the optimal rates for a static system with the average link capacities.

References

- [1] P. C. Ng and S. C. Liew, "Throughput analysis of IEEE802.11 multi-hop ad hoc networks," *IEEE/ACM Trans. Netw.*, 2007.
- [2] J. Li, C. Blake, D. S. D. Couto, H. I. Lee, and R. Morris, "Capacity of ad hoc wireless networks," in *MobiCom*. ACM, 2001.
- [3] Z. Fang and B. Bensaou, "Fair bandwidth sharing algorithms based on game theory frameworks for wireless ad-hoc networks," *IEEE INFOCOM*, 2004.
- [4] B. Yang, G. Feng, and X. Guan, "Random access in wireless ad hoc networks for throughput maximization," *International Conference on Control, Automation, Robotics and Vision*, 2006.
- [5] X. Wang and K. Kar, "Distributed algorithms for max-min fair rate allocation in aloha networks," in *Allerton Conference*, 2004.
- [6] J.-W. Lee, M. Chiang, and A. R. Calderbank, "Utility-optimal medium access control: Reverse and forward engineering," *IEEE INFOCOM*, 2006.
- [7] M. Chiang, S. Low, A. Calderbank, and J. Doyle, "Layering as optimization decomposition: A mathematical theory of network architectures," *Proceedings of the IEEE*, 2007.
- [8] X. Wang and K. Kar, "Cross-layer rate optimization for proportional fairness in multihop wireless networks with random access," *IEEE J. Sel. Areas Commun.*, 2006.
- [9] F. Kelly, A. Maulloo, and D. Tan, "Rate control in communication networks: shadow prices, proportional fairness and stability," *Journal of the Operational Research Society*, 1998.
- [10] S. Supittayapornpong and P. Saengudomlert, "Joint flow control, routing and medium access control in random access multi-hop wireless networks," *IEEE ICC*, 2009.
- [11] J. M. Mendel and K. S. Fu, *Adaptive, learning, and pattern recognition systems; theory and applications*, edited by J. M. Mendel and K. S. Fu. Academic Press, New York, 1970.
- [12] D. P. Bertsekas and R. G. Gallager, *Data Networks*, 2nd ed. Prentice-Hall, 1992.
- [13] D. O'Neill, A. Goldsmith, and S. Boyd, "Cross-layer design with adaptive modulation delay, rate, and energy tradeoffs," *IEEE GLOBECOM*, 2008.
- [14] D. P. Bertsekas, *Nonlinear Programming*. Athena Scientific, 1995.
- [15] S. Supittayapornpong, "Joint flow control, routing and medium access control in random access multi-hop wireless networks," Masters thesis, Asian Institute of Technology, 2008.
- [16] S. Boyd and L. Vandenberghe, *Convex Optimization*. Cambridge University Press, 2004.



Sucha Supittayapornpong obtained the B.Eng. degree in computer engineering from Kasetsart University, Thailand, in 2006. He then received the fellowship from Thai Government to obtain the M.Eng. degree in telecommunications from Asian Institute of Technology (AIT), Thailand, in 2008. Currently, he is a Research Associate at the Asian Institute of Technology. His research interest includes communication network

theory, resource allocation problems and distributed control algorithms in stochastic wireless networks, game theory, and network coding.



Poompat Saengudomlert received the scholarship from His Majesty the King of Thailand to obtain the B.S.E. degree in electrical engineering from Princeton University, USA, in 1996. He then received the M.S. and Ph.D. degrees, both in electrical engineering and computer science, from Massachusetts Institute of Technology (MIT), in 1998 and 2002 respectively. Currently, he is an Assistant Professor at the Asian Institute of Technology (AIT), Thailand. His research interest includes communication theory, network resource allocation problems, and optical networks.

APPENDICES

A PROOF OF THEOREM 1

We first prove Lemma 1, which is then used to prove Theorem 1. We use the procedure of proving the convexity of the log-sum-exp function in [16] to prove Lemma A.

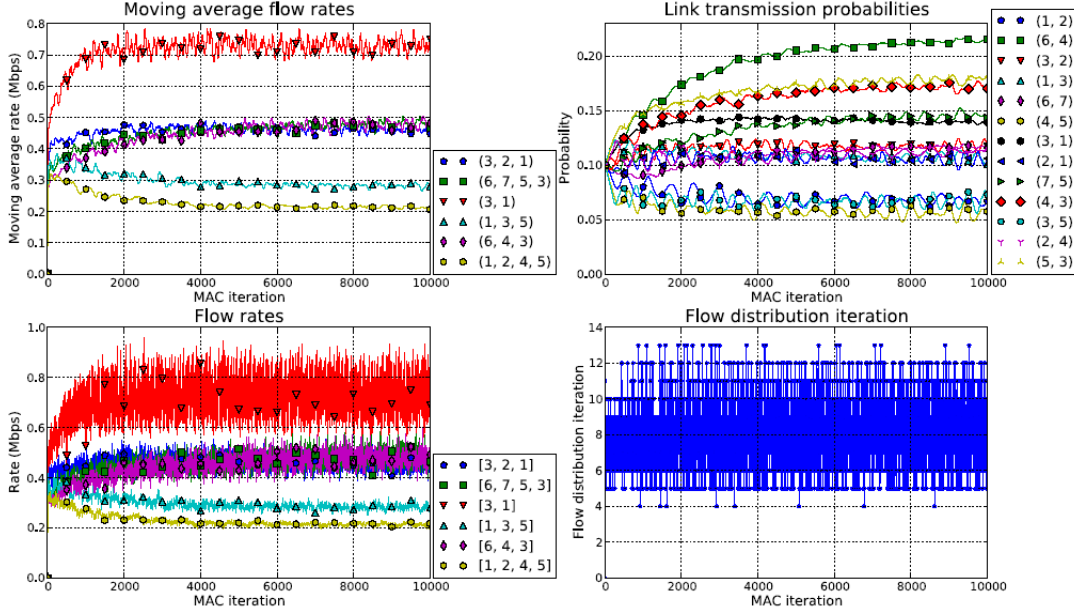


Fig.6: Complex Network Results with Link Capacity Variation

Lemma 1. Let $\mathbf{z} = (z_1, \dots, z_n)$ be an n -dimensional vector. The function $f(\mathbf{z}) = -\log \sum_{i=1}^n e^{-z_i}$ is concave in \mathbf{z} .

Proof of Lemma 1. Let $\mathbf{z} = (z_1, \dots, z_n)$, and $q(\mathbf{z}) = -f(\mathbf{z}) = \log \left(\sum_{i=1}^n e^{-z_i} \right)$

$$\begin{aligned} \frac{\partial^2 q(\mathbf{z})}{\partial z_i^2} &= \left(e^{-z_i} \sum_{k=1}^n e^{-z_k} - e^{-2z_i} \right) / \left(\sum_{k=1}^n e^{-z_k} \right)^2 \\ \frac{\partial^2 q(\mathbf{z})}{\partial z_i \partial z_j} &= \left(-e^{-z_i} e^{-z_j} \right) / \left(\sum_{k=1}^n e^{-z_k} \right)^2 \end{aligned}$$

Let $\mathbf{x} = (e^{-z_1}, \dots, e^{-z_n})$. The Hessian of $q(\mathbf{z})$ is

$$\nabla^2 q(\mathbf{z}) = \frac{1}{(\mathbf{x}^T \mathbf{1})^2} (\mathbf{x}^T \mathbf{1} \text{diag}(\mathbf{x}) - \mathbf{x} \mathbf{x}^T),$$

where $\mathbf{1}$ is the all-one vector.

To verify that $q(\mathbf{z})$ is convex, we show that $\nabla^2 q(\mathbf{z})$ is semi-positive definite. Let \mathbf{v} be any n -dimensional vector.

$$\begin{aligned} \mathbf{v}^T \nabla^2 q(\mathbf{z}) \mathbf{v} &= \frac{1}{(\mathbf{x}^T \mathbf{1})^2} [\mathbf{v}^T (\mathbf{x}^T \mathbf{1} \text{diag}(\mathbf{x})) \mathbf{v} - \mathbf{v}^T (\mathbf{x} \mathbf{x}^T) \mathbf{v}] \\ &= \frac{1}{(\mathbf{x}^T \mathbf{1})^2} \left[(\mathbf{x}^T \mathbf{1}) (\mathbf{v}^T \text{diag}(\mathbf{x}) \mathbf{v}) - (\mathbf{x}^T \mathbf{v})^T (\mathbf{x}^T \mathbf{v}) \right] \\ &= \frac{1}{(\mathbf{x}^T \mathbf{1})^2} \left[\left(\sum_{i=1}^n x_i \right) \left(\sum_{i=1}^n v_i^2 x_i \right) - \left(\sum_{i=1}^n x_i v_i \right)^2 \right] \end{aligned}$$

Let $\mathbf{a} = (\sqrt{x_1}, \dots, \sqrt{x_n})$ and $\mathbf{b} = (v_1 \sqrt{x_1}, \dots, v_n \sqrt{x_n})$ where $x_i \geq 0, i = 1, \dots, n$,

$$\mathbf{v}^T \nabla^2 q(\mathbf{z}) \mathbf{v} = \frac{1}{(\mathbf{x}^T \mathbf{1})^2} \left[\langle \mathbf{a}, \mathbf{a} \rangle \cdot \langle \mathbf{b}, \mathbf{b} \rangle - |\langle \mathbf{a}, \mathbf{b} \rangle|^2 \right].$$

From the Cauchy-Schwarz inequality, $\mathbf{v}^T \nabla^2 q(\mathbf{z}) \mathbf{v} \geq 0$ for all \mathbf{v} , so $q(\mathbf{z})$ is a convex function. Therefore, $-\log \left(\sum_{i=1}^n e^{-z_i} \right)$ is a concave function. \square

Proof of Theorem 1. Each link capacity constraint in (6) yields a convex feasible set since the left hand side is the log-sum-exp function which is convex [16], while the right hand side functions $\log p_l$ and $\log(1 - P^{(k)})$ are concave. Set \mathcal{P} is a polyhedron. The objective function is proved in Lemma 1 to be concave. Thus, problem (6) is a convex optimization problem. \square

B PROOF OF THEOREM 2

We use a similar procedure, but different in details, as in [8,10] to prove Theorem 2.

Proof of Theorem 2. Let $g_l(\mathbf{z}, \mathbf{p}) = \sum_{f \in \mathcal{R}(l)} e^{z_f} - \Phi_l(\mathbb{E}_\Psi[\mathcal{C}_l(\omega_l)], \mathbf{p})$ be a function of link capacity constraint $l \in \mathcal{L}$ in problem (7) and $\tilde{g}_l(\mathbf{z}, \mathbf{p}) = \log \left(\sum_{f \in \mathcal{R}(l)} e^{z_f} \right) - \log \Phi_l(\mathbb{E}_\Psi[\mathcal{C}_l(\omega_l)], \mathbf{p})$ be a function of link capacity constraint $l \in \mathcal{L}$ in problem (6). The utility function of both problems is denoted by $U = \sum_{s \in \mathcal{S}} -\log \left(\sum_{f \in \mathcal{F}(s)} e^{-z_f} \right)$.

Suppose $(\mathbf{z}^*, \mathbf{p}^*)$, where $\mathbf{p} = (z_f : f \in \mathcal{F})$ and $\mathbf{p} = (p_l : p \in \mathcal{L})$, satisfies the KKT conditions [14] in problem (7).

$$-\nabla U(\mathbf{z}^*) + \sum_{l \in \mathcal{L}} \lambda_l^* \nabla g_l(\mathbf{z}^*, \mathbf{p}^*) = 0 \quad (14)$$

For each $f \in \mathcal{F}$ in (14), we have

$$\begin{aligned}
& -\frac{\partial U(\mathbf{z}^*)}{\partial z_f} + \sum_{h \in \mathcal{L}} \lambda_h^* \frac{\partial g_h(\mathbf{z}^*, \mathbf{p}^*)}{\partial z_f} = 0 \\
& -\frac{\partial U(\mathbf{z}^*)}{\partial z_f} + \sum_{h \in \mathcal{J} \cap \mathcal{L}(f)} \lambda_h^* \frac{\partial g_h(\mathbf{z}^*, \mathbf{p}^*)}{\partial z_f} = \quad , \quad (15)
\end{aligned}$$

where $\mathcal{J} = \{l : g_l(\mathbf{z}^*, \mathbf{p}^*) = 0\}$ denote the set of tight constraints.

For each $l \in \mathcal{L}$ in (14), we have

$$\begin{aligned}
& -\frac{\partial U(\mathbf{z}^*)}{\partial p_l} + \sum_{h \in \mathcal{L}} \lambda_h^* \frac{\partial g_h(\mathbf{z}^*, \mathbf{p}^*)}{\partial p_l} = 0 \\
& \sum_{h \in \mathcal{J} \cap (\mathcal{I}(l) \cup \{l\})} \lambda_h^* \frac{\partial g_h(\mathbf{z}^*, \mathbf{p}^*)}{\partial p_l} = \quad . \quad (16)
\end{aligned}$$

In convex problem (6), let $\tilde{\mathcal{J}} = \{l : \tilde{g}_l(\mathbf{z}^*, \mathbf{p}^*) = 0\}$ which implies $\mathcal{J} = \tilde{\mathcal{J}}$. We take

$$\tilde{\lambda}_l^* = \lambda_l^* \sum_{m \in \mathcal{R}(l)} e^{z_m^*} = \lambda_l^* \Phi_l(\mathbb{E}_\Psi[\mathcal{C}_l(\omega_l)], \mathbf{p}^*) \quad (17)$$

for the dual variable associated with $\tilde{g}_l(\mathbf{z}, \mathbf{p})$, where $l \in \tilde{\mathcal{J}}$.

For each $f \in \mathcal{F}$ in (6), we have

$$\begin{aligned}
& -\frac{\partial U(\mathbf{z}^*)}{\partial z_f} + \sum_{h \in \mathcal{L}} \tilde{\lambda}_h^* \frac{\partial \tilde{g}_h(\mathbf{z}^*, \mathbf{p}^*)}{\partial z_f} \\
& = -\frac{\partial U(\mathbf{z}^*)}{\partial z_f} + \sum_{h \in \tilde{\mathcal{J}} \cap \mathcal{L}(f)} \tilde{\lambda}_h^* \frac{\partial \tilde{g}_h(\mathbf{z}^*, \mathbf{p}^*)}{\partial z_f} \\
& = -\frac{\partial U(\mathbf{z}^*)}{\partial z_f} + \sum_{h \in \tilde{\mathcal{J}} \cap \mathcal{L}(f)} \frac{\tilde{\lambda}_h^*}{\sum_{m \in \mathcal{F}(h)} e^{z_m^*}} \frac{\partial g_h(\mathbf{z}^*, \mathbf{p}^*)}{\partial z_f} \\
& = -\frac{\partial U(\mathbf{z}^*)}{\partial z_f} + \sum_{h \in \tilde{\mathcal{J}} \cap \mathcal{L}(f)} \lambda_h^* \frac{\partial g_h(\mathbf{z}^*, \mathbf{p}^*)}{\partial z_f} \\
& = 0. \quad (18)
\end{aligned}$$

The third equality in (18) comes from equality (17) and the last equality comes from equality (15).

For each $l \in \mathcal{L}$ in (6), we have

$$\begin{aligned}
& -\frac{\partial U(\mathbf{z}^*)}{\partial p_l} + \sum_{h \in \mathcal{L}} \tilde{\lambda}_h^* \frac{\partial \tilde{g}_h(\mathbf{z}^*, \mathbf{p}^*)}{\partial p_l} \\
& = \sum_{h \in \tilde{\mathcal{J}} \cap (\mathcal{I}(l) \cup \{l\})} \tilde{\lambda}_h^* \frac{\partial \tilde{g}_h(\mathbf{z}^*, \mathbf{p}^*)}{\partial p_l} \\
& = \sum_{h \in \tilde{\mathcal{J}} \cap (\mathcal{I}(l) \cup \{l\})} \frac{\tilde{\lambda}_h^*}{\Phi_l(\mathbb{E}_{\geq}[\mathcal{C}_{\leq}(\omega_{\leq})], \mathbf{p}^*)} \frac{\partial g_h(\mathbf{z}^*, \mathbf{p}^*)}{\partial p_l} \\
& = \sum_{h \in \tilde{\mathcal{J}} \cap (\mathcal{I}(l) \cup \{l\})} \lambda_h^* \frac{\partial g_h(\mathbf{z}^*, \mathbf{p}^*)}{\partial p_l} \\
& = 0. \quad (19)
\end{aligned}$$

The third equality in (19) comes from equality (17), and the last equality comes from equality (16).

From the results in (18) and (19), we conclude that if $(\mathbf{z}^*, \mathbf{p}^*)$ satisfies the KKT conditions in separable problem (7), then it also satisfies the KKT conditions in convex problem (6). \square